Conn / MSFC
/N-20
376 503

P8

NUMERICAL MODELING OF PRESSURIZATION OF A PROPELLANT TANK

Alok Majumdar and Todd Steadman
Sverdrup Technology
Huntsville, Al.

ABSTRACT

An unsteady finite volume procedure has been developed to predict the history of pressure, temperature and mass flow rate of the pressurant and propellant during the expulsion of the propellant from a tank. The time dependent mass, momentum and energy conservation equations are solved at the ullage space. The model accounts for the change in the ullage volume due to expulsion of the propellant. It also accounts for the heat transfer from the tank wall and propellant to the ullage gas. The procedure was incorporated in the Generalized Fluid System Simulation Program (GFSSP). The results of several test cases were then compared with a published correlation of pressurant requirements for a given displacement of propellant. The agreement between the predictions and the correlation was found to be satisfactory.

NOMENCLATURE

A	Area, ft^2
C	Ratio of wall to gas effective thermal capacity
c_p	Specific heat, Btu/lbm-R
D_{eq}	Equivalent tank diameter, ft.
Gr	Grashoff number
g	Gravitational acceleration, ft/sec^2
g_c	Conversion constant (32.174 lbm-ft/lbf-sec^2)
H	Propellant height, ft
h	Enthalpy, Btu/lbm
h_c	Heat transfer coefficient, Btu/sec-ft^2-R
J	Mechanical Equivalent of Heat (778 ft-lbf/Btu)
K_f	Flow resistance coefficient, lbf-sec^2/(lbm-$ft)^2$
K_H	Heat transfer factor
k	Conductivity, Btu/sec-ft-R
l_s	Length scale, ft
m	Resident mass, lbm
m_{wall}	Tank wall mass, lbm
$\dot{m}$	Mass flow rate, lbm/sec
Pr	Prandtl number
p	Pressure, lbf/ft^2
p_1-p_8	Constants of Epstein and Anderson's correlation
Q	Ratio of total ambient heat input to effective thermal capacitance of gas
Q_i	Heat Source, Btu/sec
$\dot{Q}$	Heat transfer rate, Btu/sec
$\dot{q}$	Ambient heat flux, Btu/sec
S	Modified Stanton number
T	Temperature, R
ΔT	Temperature difference, R
u	Velocity, ft/sec
V	Volume, ft^3
ΔV	Expelled liquid volume, ft^3
w_p	Pressurant mass, lbm
β	Coefficient of thermal expansion, 1/R
δ_{wall}	Tank wall thickness, ft
θ	Angle between branch flow velocity vector and gravity vector, deg
θ_T	Total liquid outflow time, sec
μ	Viscosity, lbm/ft- sec
ν	Kinematic viscosity, ft^2/sec
ρ	Density, lbm/ft^3

INTRODUCTION

The pressurization of a propellant tank is a complex thermodynamic process with heat and mass transfer in a stratified environment. Ring[1] described the physical processes and heat transfer correlation in his monograph. Epstein and Anderson[2] developed an equation for the prediction of cryogenic pressurant requirements for axisymmetric propellant tanks.

Draft Paper for the 37th AIAA Aerospace Sciences Meeting

Recently, Van Dresar[3] improved the accuracy of Epstein and Anderson's correlation for liquid hydrogen tanks. A computer program[4] was also developed at Marshall Space Flight Center to simulate pressurization of liquid oxygen and hydrogen tanks for testing the Space Shuttle Main Engine. This program employs a single node thermodynamic ullage model to calculate the ullage pressure based on ideal gas law, heat transfer and mixing. However, a general purpose computer program that can model flow distribution in the pressurant supply line, pressurization and heat transfer in the ullage volume and propellant flow conditions to the engine, was not available. In this paper, we describe a procedure to model pressurization and heat transfer in a propellant tank and integration of this procedure into the Generalized Fluid System Simulation Program (GFSSP)[5].

A schematic of the propellant pressurization model is shown in Figure 1. The propellant is LOX and the pressurant is helium. It is assumed that initially the ullage space was filled with helium at the propellant temperature. As the helium enters the ullage space, it mixes with cold helium and the temperature of the ullage starts to increase due to mixing and compression. Initially, the walls of the tank are at LOX temperature. Heat transfer from the ullage gas to the LOX and the tank wall starts taking place immediately after the helium begins flowing into the tank. LOX flows from the tank to the engine under the influence of ullage pressure and gravitational head in the tank.

The finite volume procedure described in this paper models the following physical processes:

a. Change in ullage and propellant volume,
b. Change in gravitational head in the tank,
c. Heat transfer from helium to LOX,
d. Heat transfer from helium to the tank wall,
e. Heat conduction between the helium exposed tank surface and the LOX exposed tank surface.

Mass transfer between the propellant and pressurant at the interface is neglected.

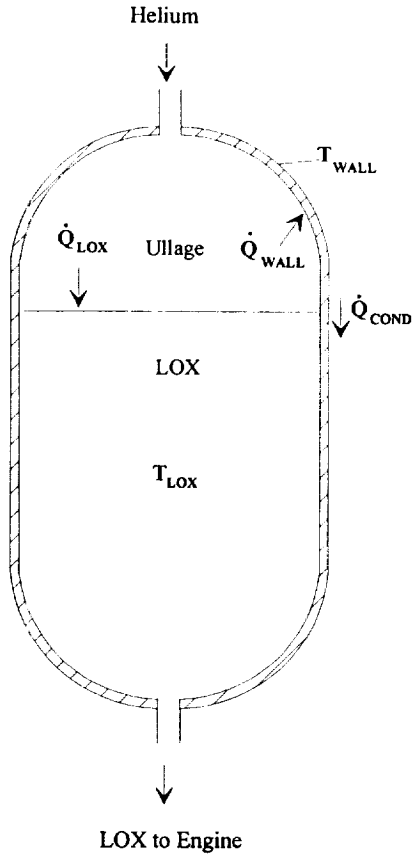

Figure 1. Schematic of LOX Tank with Helium Pressurant

GOVERNING EQUATIONS

Numerical modeling of a pressurization process requires the solution of unsteady mass, momentum and energy conservation equations in conjunction with thermodynamic equations of state. The mass, momentum and energy equations are first expressed in a finite volume form in an unstructured system of coordinates as shown in Figures 2 & 3. Figure 2 displays a schematic showing adjacent nodes, their connecting branches, and the indexing system used by GFSSP. A schematic showing a branch with upstream and downstream nodes is shown in Figure 3. In order to solve for the unknown variables, mass, energy and fluid specie conservation equations are written for each internal node and flow rate equations are written for each branch.

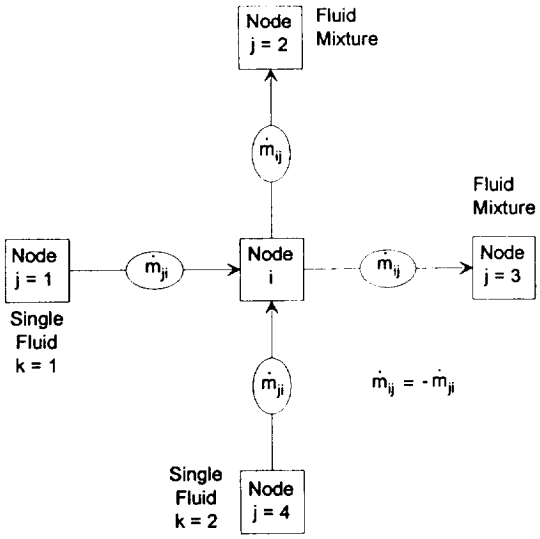

Figure 2. Schematic of GFSSP Nodes, Branches and Indexing Practice

Mass Conservation Equation

$$\frac{m_{\tau+\Delta\tau} - m_{\tau}}{\Delta\tau} = \sum_{j=1}^{j=n} \dot{m}_{ij} \qquad (1)$$

Equation 1 requires that the net mass flow from a given node must equate to rate of change of mass in the control volume.

Momentum Conservation Equation

The flow rate in a branch is calculated from the momentum conservation equation (Equation 2) which represents the balance of fluid forces acting on a given branch (Figure 3). GFSSP can model several kinds of fluid forces as shown in Equation 2.

$$\frac{\left(m u_{\tau+\Delta\tau} - m u_{\tau}\right)}{g_c \Delta\tau} + \frac{\dot{m}_{ij}}{g_c}\left(u_{ij} - u_u\right) = \left(p_i - p_j\right)A + \frac{\rho g V \cos\theta}{g_c} - K_f \dot{m}_{ij} \left|\dot{m}_{ij}\right| A \qquad (2)$$

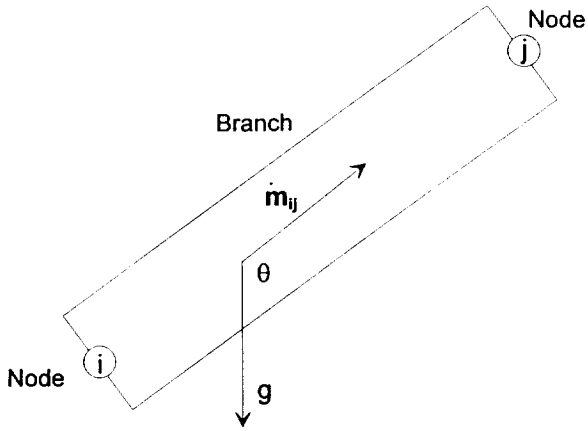

Figure 3. Schematic of a Branch Showing Gravity and Rotation

The left hand side of the momentum equation is the time dependent term and must be considered for unsteady calculations. The first term in the right hand side of the momentum equation represents the pressure gradient in the branch. The pressures are located at the upstream and downstream face of a branch. The second term represents the effect of gravity. The gravity vector makes an angle (θ) with the assumed flow direction vector. The third term represents the frictional effect. Friction was modeled as a product of K_f and the square of the flow rate and area. K_f is a function of the fluid density in the branch and the nature of the flow passage being modeled by the branch.

It may be noted that all the terms in Equation 2 are not required to be considered in modeling pressurization. The inertia and gravitational terms were not considered in Equation 2. Instead, the gravitational effect was accounted for by calculating pressure at the ullage and propellant interface as shown in Equation 8.

Energy Conservation Equation

The energy conservation equation for node i, shown in Figure 2 can be expressed mathematically as shown in Equation 3.

$$\frac{m\left(h-\frac{p}{\rho J}\right)_{\tau+\Delta\tau}-m\left(h-\frac{p}{\rho J}\right)_{\tau}}{\Delta\tau}=$$

$$\sum_{j=1}^{j=n}\left\{MAX\left[-\dot{m}_{ij},0\right]h_j-MAX\left[\dot{m}_{ij},0\right]h_i\right\}$$

$$+\frac{MAX\left[-\dot{m}_{ij},0\right]}{\left|\dot{m}_{ij}\right|}\left(p_i-p_j\right)\left(\upsilon_{ij}A\right)+Q_i \qquad (3)$$

Equation 3 shows that for transient flow, the rate of increase of internal energy in the control volume is equal to the rate of energy transport into the control volume minus the rate of energy transport from the control volume.

The MAX operator used in Equation 3 is known as an upwind differencing scheme which has been extensively employed in the numerical solution of Navier-Stokes equations in convective heat transfer and fluid flow applications. When the flow direction is not known, this operator allows the transport of energy only from its upstream neighbor. In other words, the upstream neighbor influences its downstream neighbor but not vice versa. The second term in the right hand side represents the work done on the fluid by the pressure and viscous force. The difference between the steady and unsteady formulation lies in the left hand side of the equation.

The physical processes observed in a tank pressurization system are expressed mathematically below in order to implement them in GFSSP.

Change in Ullage and Propellant Volume

Due to the discharge of propellant to the engine, resident propellant volume decreases and subsequently ullage volume increases.

$$dV_{ullage}=\frac{\dot{m}_{prop}\,\Delta\tau}{\rho_{prop}}=-dV_{prop} \qquad (4)$$

At all times the following geometric condition is satisfied:

$$V_{\text{ullage}}+V_{\text{prop}}=V_{\text{tank}} \qquad (5)$$

At each time step, propellant and ullage volumes are calculated from the following relations:

$$V_{\text{prop}}^{\tau+\delta\tau}=V_{\text{prop}}^{\tau}-dV_{\text{prop}} \qquad (6)$$

$$V_{\text{ullage}}^{\tau+\delta\tau}=V^{\tau}{}_{\text{ullage}}+dV_{\text{ullage}}^{\tau+\delta\tau} \qquad (7)$$

Change in Gravitational Head in the Tank

With the change in the propellant volume, the gravitational head (H) in the tank decreases. The pressure at the tank bottom is calculated from the following relation:

$$p_{\text{tank bottom}}=p_{\text{ullage}}+\frac{\rho_{\text{prop}}gH}{g_c} \qquad (8)$$

Heat Transfer from Helium to LOX

The heat transfer from the ullage gas to the LOX is expressed as:

$$\dot{Q}_{LOX}=\left[h_cA\right]_{ullage-LOX}(T_{He}-T_{LOX}) \qquad (9)$$

It has been assumed that the heat transfer is due to natural convection with the heat transfer coefficient expressed as:

$$h_c=K_HC\frac{k_f}{L_s}X^n \qquad (10)$$

where,

$$X=(Gr)(\mathrm{Pr}) \qquad (11)$$

$$Gr=\left(\frac{l^3\rho_f^2g\beta_f|\nabla T|}{\mu_f^2}\right) \qquad (12)$$

$$\mathrm{Pr}=\left(\frac{c_{pf}\mu_f}{k_f}\right) \qquad (13)$$

Gr and Pr are the Grashoff number and the Prandtl number of the ullage gas respectively.

According to Ring[1] C=0.27, n=0.25, and K_H (heat transfer adjustment factor) is set to 1.0. The length scale in Equation 12 is set to the diameter of the tank.

Heat Transfer from Ullage Gas to Wall

The heat transfer from the helium to the wall is expressed as:

$$\dot{Q}_{wall} = \left[h_c A\right]_{ullage-wall}(T_{He} - T_{wall}) \qquad (14)$$

It has also been assumed that the heat transfer is due to natural convection and the heat transfer coefficient is expressed by Equations 10 and 11. According to Ring[1] C=0.54 and n=0.25 for this case. The diameter of the tank was again considered to be the length scale used in the heat transfer correlation.

Transient Heat Transfer in the Tank

Wall temperature has been calculated from a transient heat conduction equation:

$$m_{\text{wall}}\, c_{\text{p,wall}} \frac{\partial T_{\text{wall}}}{\partial \tau} = \dot{Q}_{\text{wall}} - \dot{Q}_{\text{cond}} \qquad (15)$$

where

$$m_{\text{wall}} = \rho_{\text{wall}} A_{\text{helium to wall}} \delta_{\text{wall}} \qquad (16)$$

$$\dot{Q}_{\text{cond}} = k_{\text{tank}} A_{\text{cond}} (T_{\text{wall}} - T_{\text{lox}}) / (H/2) \qquad (17)$$

The model accounts for the change in the heat transfer area as the ullage volume increases during the pressurization process. However, area was calculated assuming a cylindrical shaped tank. The tank diameter has been assumed to be the length scale in both heat transfer correlations [Equations 9 and 14].

GFSSP TEST MODEL

A 5-node pressurization system GFSSP test model, as shown in Figure 4, was developed to test the implementation of the pressurization option. Helium at 95 psia and 120° F enters the ullage space through an orifice. The ullage space is initially filled with helium at -265° F. Node 2 represents the ullage space. A pseudo boundary node (Node 3) has been introduced to exert ullage pressure on the propellant tank. The pressure at the pseudo boundary node is calculated from the ullage pressure and gravitational head and is the driving force to supply the propellant to the engine. This pressure is calculated at the beginning of each time step. Branch 34 represents the propellant tank and Branch 45 represents the line to the engine. In this test model, the engine inlet pressure was set at 50 psia.

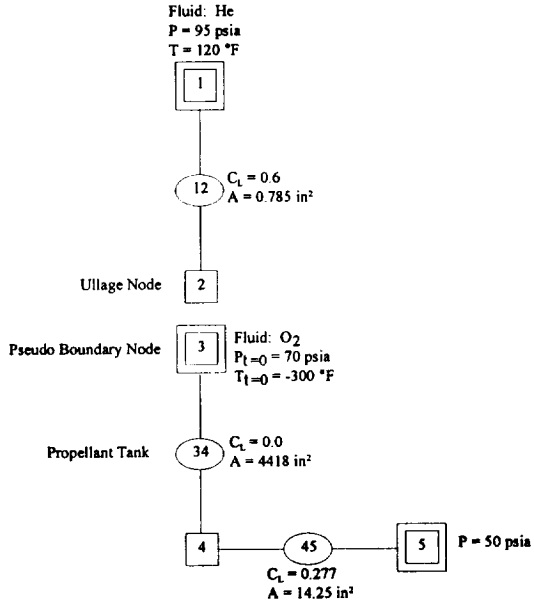

Figure 4. A Simple Pressurization System Test Model

RESULTS AND DISCUSSION

The pressurization system transient test model was run for 60 seconds with 0.1 second time step. The model run time was approximately 122 seconds using a 200 MHz Pentium II with Windows NT and 32 megabytes of RAM.

Figure 5 shows both the ullage pressure and tank bottom pressure histories for the test model. After an initial pressure rise due to a "ramping up" transient effect, both pressures maintain an approximate steady state value for the remainder of the run. It should be noted that tank bottom pressure was calculated (Equation 8) by adding ullage pressure with pressure due to gravitational head. Figure 5 shows that as the gravitational head decreases, the ullage and tank bottom pressures slowly begin to converge.

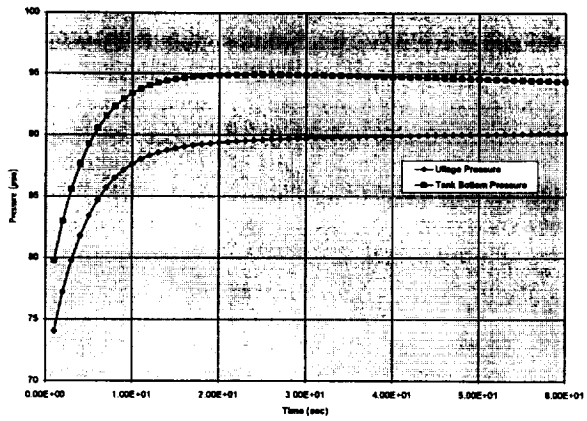

Figure 5. Ullage and Tank Bottom Pressure History

Figure 6 shows the histories for the ullage temperature and the tank wall temperature. Figure 6 shows that the tank wall temperature only rises eight degrees over the course of the model run, revealing that the 120 °F helium gas entering the tank has an almost negligible effect on the tank wall. This is because the heat gained by the wall is conducted to the portion of the tank which is submerged in LOX, which dampens the temperature rise of the tank. On the other hand, the ullage temperature, initially at LOX temperatures, rises over a hundred degrees as the helium gas pressurizes the tank. This large temperature rise is primarily due to the mixing of hot helium gas with the relatively cold gas initially present in the ullage.

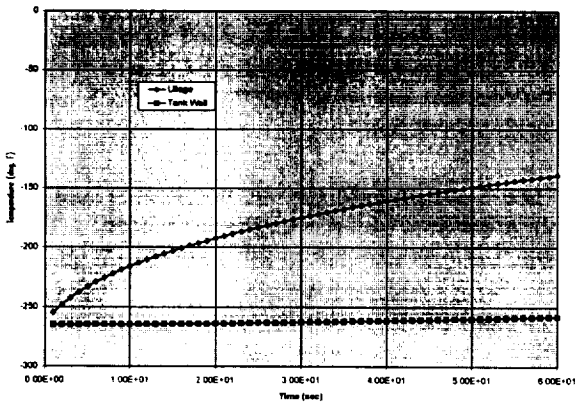

Figure 6. Ullage and Tank Wall Temperature History

Figure 7 shows the ullage and propellant volume histories for the test model. Approximately 130 ft^3 of propellant was discharged from the tank during the pressurization process.

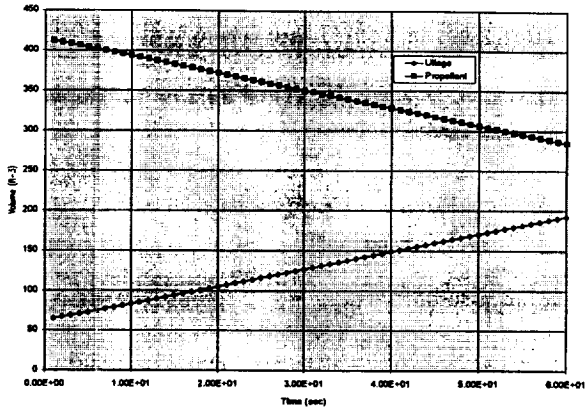

Figure 7. Ullage and Propellant Volume History

Helium flow rate into the tank is shown in Figure 8. The helium flow rate was found to drop over the duration of the run as it approached a steady state mass flow rate. LOX flow rate into the engine is shown in Figure 9. The LOX flow rate curve mirrored the ullage and tank bottom pressure curves, rising through an initial start transient to a steady state value for most of the run.

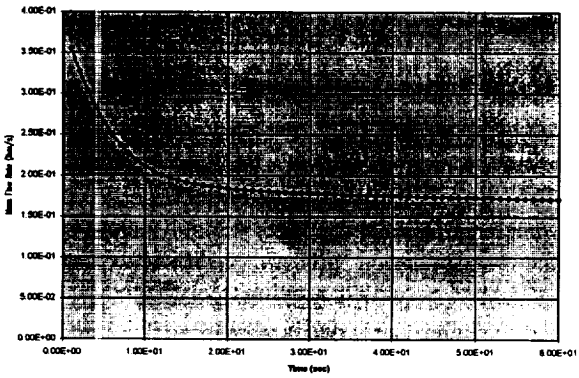

Figure 8. Helium Flow Rate into the Tank

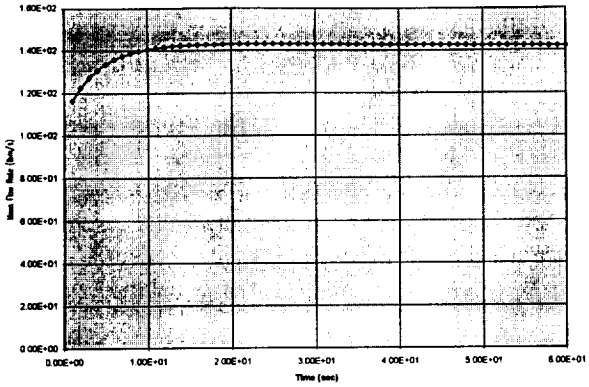

Figure 9. LOX Flow Rate to the Engine

As a validation, finite volume procedure predictions were compared with a published correlation of pressurant requirements for a given displacement of propellant as published by Epstein and Anderson [2]. The correlation calculates the collapse factor, which is defined by Van Dresar [3] as a ratio of the actual pressurant consumption to an ideal pressurant consumption where no heat or mass transfer from the pressurant occurs. This correlation takes the form shown in Equations 18 through 22.

$$\frac{w_p}{w_p^0} = \left\{ \begin{array}{l} \left(\frac{T_0}{T_s} - 1\right)\left[1 - \exp\left(-p_1 C^{p_2}\right)\right] \\ \times \left[1 - \exp\left(-p_3 S^{p_4}\right)\right] + 1 \end{array} \right\} \times \exp\left[- p_5 \left(\frac{1}{1+C}\right)^{p_6} \left(\frac{S}{1+S}\right)^{p_7} Q^{p_8} \right] \quad (18)$$

where

$$w_p^0 = \rho_G^0 \Delta V \quad (19)$$

$$C = \frac{\left(\rho c_p^0 \delta\right)_{wall}}{\left(\rho c_p\right)_G^0 D_{eq}} \frac{T_s}{T_0} \quad (20)$$

$$S = \frac{h_c \theta_T}{\left(\rho c_p\right)_G^0 D_{eq}} \frac{T_s}{T_0} \quad (21)$$

$$Q = \frac{\dot{q} \theta_T}{\left(\rho c_p\right)_G^0 D_{eq} T_0} \quad (22)$$

Van Dresar [3] later modified this correlation by redefining D_{eq} as shown in Equation 23.

$$D_{eq} = 4 \frac{\Delta V}{A_{sw}} \quad (23)$$

The validation exercise consisted of comparing pressurant mass predictions for four different propellants with helium as the pressurant in each case. The four propellants used were oxygen, hydrogen, nitrogen and fluorine. Table 1 shows the results of this validation exercise. The comparison ranges from 6.31% for the hydrogen propellant case to 18.12% for the oxygen propellant case. It is observed that GFSSP predicts lower mass in the ullage for oxygen, nitrogen and fluorine. The primary cause of the discrepancy between comparisons is due to the assumption of no mass transfer in the finite volume procedure. However, the comparison is better for hydrogen which is lighter than the other propellants considered in this study.

Table 1. Pressurization Validation Results

Propellant	GFSSP Pressurant Mass Prediction (lbm)	Epstein Correlation Pressurant Mass Prediction (lbm)	Discrepancy (%)
Oxygen	32.36	39.52	18.12
Hydrogen	39.07	36.75	6.31
Nitrogen	16.4	18.97	13.55
Fluorine	23.71	28.4	16.51

CONCLUSIONS

A finite volume procedure has been developed to model the pressurization of a propellant tank. A simple model has been developed to test the numerical stability of the algorithm and physical plausibility of the results. The prediction of pressurant requirements compared favorably with Epstein's correlation.

ACKNOWLEDGEMENT

This work was performed for NASA/MSFC under contract NAS8-40836, Task Directive 371-302, to support the design of Propulsion Test Article 1(PTA1) with Dr. Charles Schafer of MSFC as the Task Initiator. The authors would like to express

their appreciation to Mr. David Seymour and Ms. Kimberly Holt of MSFC for their constructive review and comments during the course of this work. The authors would also like to acknowledge Mr. Tom Beasley and Karl Knight of Sverdrup Technology for reviewing this paper.

REFERENCES

1. Ring, Elliot, "Rocket Propellant and Pressurization Systems", Prentice Hall, 1964.
2. Epstein, M., and Anderson, R.E., "An Equation for the Prediction of Cryogenic Pressurant Requirements for Axisymmetric Propellant Tanks," *Advances in Cryogenic Engineering*, Vol. 13, Plenum, New York, 1968, pp. 207-214.
3. Van Dresar, Neil T., "Prediction of Pressurant Mass Requirements for Axisymmetric Liquid Hydrogen Tanks", *Journal of Propulsion and Power*, Vol. 13, No. 6, 1997, pp. 796-799.
4. Flachbart, Robin, A Computer Program entitled "TTBSIM" for simulating Tank Pressurization for Technology Test Bed at Marshall Space Flight Center, June 1997.
5. Majumdar, A, Bailey, J. W., Schallhorn, P., Steadman, T., "A Generalized Fluid System Simulation Program to Model Flow Distribution in Fluid Networks", Sverdrup Technology Report No. 331-201-97-005, Contract No. NAS8-40836, 1997.